



**[biblio.ugent.be](https://biblio.ugent.be)**

The UGent Institutional Repository is the electronic archiving and dissemination platform for all UGent research publications. Ghent University has implemented a mandate stipulating that all academic publications of UGent researchers should be deposited and archived in this repository. Except for items where current copyright restrictions apply, these papers are available in Open Access.

This item is the archived peer-reviewed author-version of:

Plant-wide investigation of sulfur flows in a water resource recovery facility (WRRF)

Forouzanmehr, F., Le, Q.H., Solon, K., Maisonnave, V., Daniel, O., Buffiere, P., Gillot, S., Volcke, E.I.P.

In: Science of The Total Environment, 801, 149530, 2021.

**To refer to or to cite this work, please use the citation to the published version:**

Forouzanmehr, F., Le, Q.H., Solon, K., Maisonnave, V., Daniel, O., Buffiere, P., Gillot, S., Volcke, E.I.P. (2021). Plant-wide investigation of sulfur flows in a water resource recovery facility (WRRF). Science of the Total Environment, 801, 149530.  
[doi.org/10.1016/j.scitotenv.2021.149530](https://doi.org/10.1016/j.scitotenv.2021.149530).

**Plant-wide investigation of sulfur flows in a water resource recovery facility (WRRF)**

F. Forouzanmehr <sup>a, b, c</sup>, Q. H. Le <sup>a</sup>, K. Solon <sup>a</sup>, V. Maisonnave <sup>b</sup>, O. Daniel <sup>b</sup>, P. Buffiere <sup>c</sup>, S. Gillot <sup>d</sup>, E. I. P. Volcke<sup>a,\*</sup>

<sup>a</sup> Department of Green Chemistry and Technology, Ghent University, Belgium

<sup>b</sup> Veolia Recherche & Innovation (VeRI), Maisons-Laffitte, France

<sup>c</sup> Univ Lyon, INSA-Lyon, Laboratory of Waste Water Environment and Pollutions (DEEP) EA 7429, F-69621  
Villeurbanne, France

<sup>d</sup> INRAE, UR REVERSAAL, F-69625, Villeurbanne Cedex, France

\* Corresponding author. E-mail address: [Eveline.Volcke@UGent.be](mailto:Eveline.Volcke@UGent.be) (E.I.P. Volcke)

## Abstract

Even though sulfur compounds and their transformations may strongly affect wastewater treatment processes, their importance in water resource recovery facilities (WRRF) operation remains quite unexplored, notably when it comes to full-scale and plant-wide characterization. This contribution presents a first-of-a-kind, plant-wide quantification of total sulfur mass flows for all water and sludge streams in a full-scale WRRF. Because of its important impact on (post-treatment) process operation, the gaseous emission of sulfur as hydrogen sulfide ( $\text{H}_2\text{S}$ ) was also included, thus enabling a comprehensive evaluation of sulfur flows. Data availability and quality were optimized by experimental design and data reconciliation, which were applied for the first time to total sulfur flows. Total sulfur flows were successfully balanced over individual process treatment units as well as the plant-wide system with only minor variation to their original values, confirming that total sulfur is a conservative quantity. The two-stage anaerobic digestion with intermediate thermal hydrolysis led to a decreased sulfur content of dewatered sludge (by 36%). Higher (gaseous)  $\text{H}_2\text{S}$  emissions were observed in the second-stage digester (42% of total emission) than in the first one, suggesting an impact of thermal treatment on the production of  $\text{H}_2\text{S}$ . While the majority of sulfur mass flow from the influent left the plant through the treated effluent (> 95%), the sulfur discharge through dewatered sludge and gaseous emissions are critical. The latter are indeed responsible for odour nuisance, lower biogas quality,  $\text{SO}_2$  emissions upon sludge combustion and corrosion effects.

**Keywords:** *Wastewater treatment, Sulfur mass flows, Experimental design, Plant-wide data analysis, Data reconciliation*

## 1. Introduction

Wastewater treatment plants (WWTPs) are no longer viewed solely for protecting the aquatic environment and ensuring the required effluent quality in terms of chemical oxygen demand and nutrients (nitrogen and phosphorus), but instead, they are increasingly regarded as water resource recovery facilities (WRRFs) with growing interest for energy and resource recovery (Hao et al., 2019; Solon et al., 2019a). The energy recovery is mostly in the form of methane-containing biogas produced from anaerobic digestion (Guest et al., 2009) that can be combusted on-site for heat and electricity generation or cleaned-up and sold (Puchongkawarin et al., 2015). The resource recovery in WRRFs typically relates to phosphorus and nitrogen recovery which are of the interest due to limited resource of phosphorus and substantial energy requirement for nitrogen production and greenhouse gas emission, respectively (Galloway and Cowling, 2002; Marti et al., 2008; Mihelcic et al., 2011; Puchongkawarin et al., 2015).

Sulfur cycle influences both energy recovery and resource recovery, in addition to safety concerns. The methane production can be negatively affected by the competition of sulfate-reducing bacteria and methanogens for hydrogen and acetate (Harada et al., 1994; Muyzer and Stams, 2008; Visser et al., 1993). Moreover, sulfide, especially in undissociated form, has an inhibitory effect on anaerobes (e.g. methanogens and acetogens) which are involved in the anaerobic digestion of sludge (Appels et al., 2008; Chen et al., 2008; Guerrero et al., 2016; Yang et al., 2016). Generation of high concentration of hydrogen sulfide ( $H_2S$ ) in biogas necessitates further processing of biogas before co-generation due to its corrosive properties (Tchobanoglous et al., 2003); hence lowering the profitability of produced biogas.

The sulfur cycle is strongly linked to that of other elements such as nitrogen and phosphorus through various biological and (geo)chemical processes (Lomans et al., 2002; Puyol et al., 2017; Solon et al., 2019b). These interactions include the reoxidation of iron sulfide in the aeration tank (Schipper and Jørgensen, 2002) and subsequent precipitation of phosphate with released iron (Ge et al., 2013; Gutierrez et al., 2010), effects on the performance of enhanced biological phosphorus removal (EBPR) process as a result of SRB activity (Baetens et al., 2001; Wanner et al., 1987; Yamamoto-Ikemoto et al., 1994) and exposure to high sulfide concentration (Rubio-Rincón et al., 2017a, 2017b; Saad et al., 2017), the release of ferric ions from ferric phosphate precipitates to precipitate with the sulfide formed in anaerobic digester (due to higher affinity of sulfide for iron than for phosphate) which ultimately lowers  $H_2S$  emission from digesters (Ge et al., 2013; Roussel and Carliell-Marquet, 2016), and the simultaneous sulfide oxidation and nitrate reduction known

as autotrophic denitrification which has been applied in the development of new processes e.g. SANI (Lau et al., 2006; Wang et al., 2009).

The potential emission of volatile sulfur compounds (VSCs) has given rise to public concern about WRRFs in the vicinity of residential areas (Frechen, 1988; Gostelow et al., 2001; Lebrero et al., 2013). The main volatile sulfur compounds are  $\text{H}_2\text{S}$ , methyl mercaptan (MM), dimethyl sulfide (DMS) and dimethyl disulphide (DMS) (Bazemo et al., 2021).  $\text{H}_2\text{S}$  has traditionally been used as a surrogate for odour emissions (Gostelow et al., 2001). In a recent study on 6 WRRFs (Fisher et al., 2018),  $\text{H}_2\text{S}$  was confirmed to be the most important volatile sulfur compound in terms of concentration as well as the most dominant odorant based on odour activity value (OAVs). In the latter study, methyl mercaptan was also found to be sensorially important due to low odour detection threshold (ODT). Consequently, the odour collection and treatment are becoming more and more required in WRRFs. Odorous emission occurs in two categories of process units (Gostelow et al., 2001); process units that only promote emission of previously formed odorous compounds e.g. wastewater inlet works and process units in which both formation and emission occur e.g. primary settling/thickening. Based on information from literature, the two important sources of emission are primary treatments and sludge treatment units (Dincer and Muezzinoglu, 2008; Jiang et al., 2017; Lebrero et al., 2011; Ras et al., 2008), whereas the biological treatment units (aerobic, anoxic tanks and secondary settling) were shown to be less emissive (Frechen, 2004), since hydrogen sulfide is biologically and chemically oxidised to sulfate in these oxidative environments.

Despite its importance, less attention has been given to the sulfur cycle when it comes to full-scale studies. Full-scale sulfur studies are challenging because of the multiphase nature of sulfur (i.e. liquid, solid and gaseous states), the wide range of sulfur species and redox states, ranging from sulfide (-2) to sulfate (+6), interrelated conversions and transformations, difficulties in monitoring gaseous emissions from process units (e.g. open surface of settling tanks) and challenges in sulfur analysis in liquid samples because of the loss of  $\text{H}_2\text{S}$  due to volatilisation during sample collection.

A key step towards enhancing sulfur studies in WRRFs is quantifying the distribution of sulfur in a plant-wide level as it is helpful for: (i) identifying key sulfur flows, (ii) enabling quantitative comparison of sulfur flows in different streams, (iii) identifying the influence of process units on sulfur flows, (iv) identifying key spots for sulfur recovery and/or reducing the negative effects of sulfur and (v) facilitating the correct design of odour collection and treatment facilities as data is typically scarce.

In literature, several studies partly addressed the distribution of sulfur flows in the sludge treatment units, providing valuable information in regard to the effect of process units on the sulfur flows (Dewil et al., 2008, 2009; Fisher et al., 2017; Yoshida et al., 2015). The role of secondary sludge thickening in reducing sulfur flows towards successive process treatment was highlighted by Dewil et al. (2008, 2009), who traced flows of total sulfur through four WWTPs. By mapping the sulfur flows in the sludge processing of six WWTPs with different configurations, Fisher et al. (2017) noted higher sulfur recovery in sludge at sites with a combination of primary and secondary treatments, attributing it to the incorporation of sulfate into the biomass and capturing and sending more solids to the sludge processing. Other factors increasing sulfur recovery were higher efficiency of the primary settling tank, thickening and dewatering units, as well as higher iron content in the digesters. Yoshida et al. (2015) traced mass flows of 32 elements including sulfur throughout a WRRF. In their study, gaseous emissions were not measured but instead calculated from mass balances, leading to high uncertainties of gaseous streams, often above 100%. Nevertheless, the comprehensive sulfur management in WRRFs requires a plant-wide level approach as most process units are more or less affected by the sulfur cycle and because sulfur can be distributed to water, sludge and gaseous streams. To our knowledge, quantification of total sulfur mass flows in plant-wide level with simultaneous measurements in water, sludge and gaseous streams has not yet been performed at WRRFs.

In the process of tracking sulfur flows, Fisher et al. (2017) mentioned the limitations in data availability and quality, which highlights the importance of thorough experimental design and data reconciliation for tracking substance flows (Behnami et al., 2016; Meijer et al., 2002, 2015; Puig et al., 2008). To address this issue, Le et al. (2018) developed a mass balanced-based experimental design procedure which provides Pareto-Optimal solutions (i.e. measurement layouts) in terms of their cost and accuracy of key variables. These solutions guarantee the subsequent reconciliation of the collected dataset through data reconciliation. Reconciliation, in this context, means that the value of variables, regardless of being measured or not, would be calculated from other measurements based on the constraints in the form of mass balances. This methodology is applied to a WRRF to trace sulfur flow to ensure the quality of data but also prevent trivial measurements.

This study aims to quantify the distribution of sulfur flow in a municipal WRRF, addressing all process units in the water line and sludge line as well as taking into account water, sludge and gaseous streams. The case study plant had an innovative configuration in sludge treatment by having two-stage digestion with intermediate thermal treatment, which enabled the evaluation of sludge post-treatment processes on sulfur flow distributions. The total sulfur mass

flows were obtained following three steps: experimental design, data collection and data reconciliation. The sulfur flows throughout the plant were compared, identifying key flows and how they are influenced by unit processes.

## 2. Material and methods

### 2.1. WRRF under study

The municipal WRRF under study (**Fig. 1**) has a capacity of 620,000 P.E. (average daily flow during the measuring campaign:  $137151 \pm 12573 \text{ m}^3 \cdot \text{d}^{-1}$ ) and comprises pre-treatment, secondary treatment and sludge treatment. Pre-treatment process consists of screening and grit and grease removal, followed by primary settling equipped with lamella plates. The primary settling effluent is sent to secondary treatment in an integrated fixed-film activated sludge (IFAS) process for the removal of carbon, nitrogen and phosphorus. The secondary treatment is realized in seven compartments: a pre-anoxic reactor, an anaerobic reactor, an anoxic reactor, an aerated reactor with carriers, a de-oxygenation reactor without aeration, a post-anoxic reactor with methanol addition and a post-aeration tank with aluminium chloride addition for chemical phosphorus removal. Effluent from the secondary clarifier passes through filtration as a tertiary treatment before final discharge. During intense rain events, the potential surplus influent wastewater flow is directed towards the rain treatment line which is based on chemically enhanced primary treatment.

Primary and secondary sludge are pumped to the gravity thickener and dynamic thickener (rotary drums), respectively. The thickened primary and secondary sludge as well as a small fraction of the thickened sludge originating from the rain treatment line are mixed in a sludge buffer tank. Mesophilic anaerobic digestion is performed in two stages, the first of which takes place in two parallel units. The first-stage digested sludge is pre-dewatered by a centrifuge and sent to a thermal hydrolysis unit ( $165^\circ\text{C}$ , 8 bar, 30 minutes). The thermally treated sludge is diluted and cooled by adding some treated effluent. The subsequent second stage digestion is performed in a single unit. All three digester tanks have the same volume ( $6100 \text{ m}^3$ ). The average sludge retention time of first stage and second stage are 20 and 30 days, respectively. These digesters are equipped with air injection to the headspace for biological removal of hydrogen sulfide from biogas (microaeration process). The second-stage digested sludge is sent to a storage tank and then dewatered by a centrifuge. The filtrate of primary and secondary thickening, centrate of pre-dewatering and post-dewatering as well as the reuse water, which is used for internal usages e.g. cleaning, return to the upstream of pre-treatment.

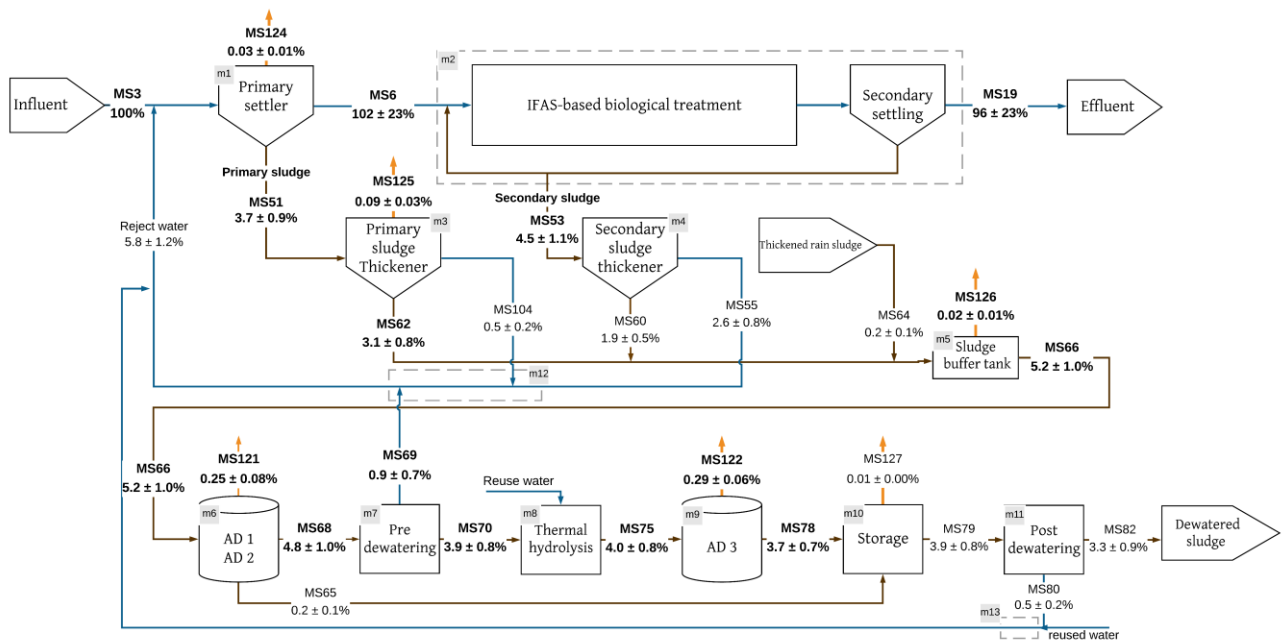


**Fig. 1:** Simplified process flow diagram of the WRRF under study. The total sulfur mass flows in the streams are given as a percentage of the total sulfur mass flow in the influent. Water streams, sludge streams and gas streams are shown in blue, brown and yellow lines, respectively. The key variables which need to be reconciled to fulfil the main goal of the measuring campaign are given in bold. The mass balances (#m) were derived around individual and/or combined process units; in the latter case, the boundaries are shown by dashed boxes.



## 143 2.2. Measurement campaign

144 The measurement campaign was performed during two weeks in June 2019. The measurement layout in this campaign  
145 was selected by following an experimental design procedure (Section 2.3.1). The sampling method in the water line  
146 and sludge treatment lines were composite samples and grab samples, respectively. The water and sludge samples were  
147 analysed for total sulfur ( $\text{g S}\cdot\text{m}^{-3}$ ) using inductively coupled plasma optical emission spectrometry (ICP-OES)  
148 following NF EN ISO 11885 standard. An overview of the measurements including the sampling points and the number  
149 of samples is provided in section B2 in the Supplementary Information (SI).

150 Determination of gaseous sulfur from unit processes where high emission levels were expected was done by monitoring  
151 the emitted hydrogen sulfide as the dominant gaseous sulfur species. Other volatile sulfur compounds in the gas phase  
152 were assumed negligible, such that hydrogen sulfide was considered as an approximation of total sulfur in the gas  
153 phase. This assumption is in accordance with previous studies that hydrogen sulfide is the most dominant and  
154 prevailing gaseous sulfur species in WRRFs (Fisher et al., 2018; Gostelow et al., 2001).

155 The studied process units included primary settler, primary thickener, sludge buffer tank, anaerobic digesters and  
156 digested sludge storage tank. The selection of these units was based on literature review of emissive units in WRRFs,  
157 consulting with practitioners on site about units with odour and corrosion issues and previous experiences with other  
158 WRRFs. Although some emission could occur from other process units, their contribution is expected to be negligible  
159 compared to the emission from the seven most emissive units covered in this study. Sulfur mass flow data for the  
160 biogas of anaerobic digesters were collected from the supervisory control and data acquisition system (SCADA), which  
161 was programmed to provide sulfur mass flow data based on the measured airflow rate and  $\text{H}_2\text{S}$  concentration of biogas.  
162 The  $\text{H}_2\text{S}$  concentration of biogas was analysed by Awiflex gas analyser (Awite Bioenergie GmbH, Germany). For the  
163 other process units, which were completely covered, the  $\text{H}_2\text{S}$  concentration was measured in the ventilation pipes. Two  
164 types of  $\text{H}_2\text{S}$  meters were installed in parallel to ensure measurement reliability: a myKlearSens  $\text{H}_2\text{S}$  meter (standard  
165 range 0-200 ppm, also covering peaks up to 1000 ppm) (Klearios, France) and an OdaLog<sup>®</sup>  $\text{H}_2\text{S}$  meters (0-200ppm)  
166 (App-Tek, Australia). Continuous measurements of gaseous  $\text{H}_2\text{S}$  were performed with a frequency of 5 minutes over  
167 two weeks. In order to obtain the mass flow, airflow rates in the ventilation pipes were measured on the first day of  
168 the campaign using pitot tube, hot-wire and helix anemometers. The flow rates of the water and sludge streams were  
169 collected from the SCADA system.

## 170    **2.3. Quantification of total sulfur mass flows**

171    The main goal of this study was the quantification of the total sulfur flows in the WRRF. Experimental design was  
172    applied to select sampling points that guaranteed obtaining a reliable and adequate data set through subsequent data  
173    reconciliation. The experimental design and data reconciliation procedures were based on the principle of mass  
174    conservation, the conservative quantity being total sulfur.

### 175    **2.3.1. Experimental design**

176    Experimental design was applied to choose the measurement layout to obtain the required information with a minimal  
177    number of measurements and maximum accuracy. The step-wise experimental design procedure of Le et al. (2018)  
178    (see section A1 in SI) was followed to this end. This experimental design procedure evaluates possible measurement  
179    layouts through redundancy analysis and identifies the list of optimum solutions in terms of cost and accuracy that  
180    guarantee the reconciliation of key variables, and thus fulfil the main goal of the measuring campaign. Key variables  
181    may be measured or not. Reconciliation means that the value of key variables is calculated from other, measured  
182    variables, based on the constraints in the form of mass balances. The applied experimental design procedure consists  
183    of 7 steps, which are detailed below.

184    As a first step, the main goal was translated into key variables, in this case 17 total sulfur mass flows (section A3 in  
185    SI). The key variables covered water, sludge and gas lines and were selected as streams which were expected to contain  
186    significant sulfur loads and/or to be involved in important sulfur conversions, based on information from literature and  
187    expert knowledge. Gas streams which were expected to contain a significant amount of sulfur were added *a priori* as  
188    measured variables (6 streams, see **Fig. 1** or **Table A5** in SI). Five of them were taken up as key variables (see **Table**  
189    **A3** in SI). Second, mass balances for total sulfur flows were defined around individual and/or combined process units  
190    (section A4 in SI). Third, data inventory was done based on historical data and expert knowledge to estimate the mean  
191    values, expected uncertainties and the measurement cost of potential additionally measured variables (section A5 in  
192    SI). The potential additional measured variables were limited to total sulfur concentrations. The flow rate  
193    measurements were limited to ones already installed in the plant (30 out of 33 flows were measured). The experimental  
194    design procedure then performed a redundancy analysis (step 4-6 of **Fig. A1** in SI) and solved a multi-objective  
195    optimization problem (step7), minimising the cost (number of additional measurements) and maximizing the accuracy  
196    (precision improvement of key variables). The results were visualised in a Pareto-optimal front that was used to select  
197    the measurement layout, i.e. the set of additional measured variables.

### 198 2.3.2. Data reconciliation

199 The collected dataset was subject to the mass balance-based bilinear data reconciliation procedure of Le, (2019, see  
200 section B1 in SI). Provided there is sufficient redundancy in the dataset, this procedure provides better estimates for  
201 the key variables in terms of their mean value and uncertainty. In addition, the applied procedure performs several  
202 gross error detection techniques. The procedure can be divided into three steps, input preparation, data reconciliation  
203 and gross error detection, which are detailed below.

204 The data reconciliation procedure required three input information, namely, key variables, mass balances and pre-  
205 processing of the raw measurements. The key variables and mass balances were the same as for the experimental  
206 design step. Pre-processing of the raw dataset involves listing the mean values and uncertainty of the measured  
207 variables. Determination of variable uncertainties was done taking into account the measurement errors, standard error  
208 and sampling method (see section B2 in SI).

209 The extent of data reconciliation was assessed based on two indicators, namely the correction factor and the precision  
210 improvement. The correction factor ( $\Delta_x$ ) reflects the accuracy of measurements and is defined as the ratio of the  
211 difference between the mean of the measurement ( $mean(x)$ ) and the mean of the reconciled value ( $mean(\bar{x})$ ) to the  
212 mean of the measurement, expressed in percentage.

$$\Delta_x = \frac{mean(x) - mean(\bar{x})}{mean(x)} \quad \text{Eq.1}$$

213 The precision improvement ( $i_x$ ), also known as the effect of balancing (van der Heijden et al., 1994), is defined as the  
214 ratio of the difference between the variance of the measurement ( $var(x)$ ) and the variance of the reconciled value  
215 ( $var(\bar{x})$ ) to the variance of the measurement, expressed in percentage. The higher the precision improvement, the  
216 more accurate the value of the key variable is known after data reconciliation.

$$i_x = \frac{var(x) - var(\bar{x})}{var(x)} \times 100 \quad \text{Eq.2}$$

217 Furthermore, the dataset was checked for gross errors by testing the dataset against alternative hypotheses: (1) the null  
218 hypothesis,  $H_0$ , that no gross error is present, and (2) the alternative hypothesis,  $H_1$ , that gross errors are present. Three  
219 tests were incorporated in the data reconciliation procedure, namely, global test, nodal test and measurement test. The

global test provides a general signal if there is a potential gross error in the data set, the nodal test narrows this down to individual constraints and the measurement test suggests potential suspected measurements with gross errors. Details of these tests can be found in Le (2019).

### 3. Results and discussion

#### 3.1. Experimental design- selection of measurement layout

Key variables were selected from the water line, sludge line and gas streams (**Table A3** in SI). The experimental design evaluated whether or not the main goal, subsequent reconciliation of the key variables, was achievable for the given set of measurements and potential additionally measured variables (section A6 in SI). Based on the process flow sheet and the initially available measurements, 17 potentially additional sampling points for the measurement of total sulfur were identified, corresponding to  $2^{17} = 131072$  potential measurement layouts, i.e. combinations of potential additional sampling points. All measurement layouts were evaluated by the experimental design procedure. From all evaluated combinations, 3534 measurement layouts resulted in the reconciliation of key variables and thus were considered as solutions, seven of them were optimal solutions, lying on the Pareto-front (**Fig. 2**, details of Pareto-Optimal solutions including the sampling points of each solution are given in section A6 in SI). Each of these solutions is a measurement layout (= combination of possible additional measurements) that guarantees the improvement of defined key variables and is Pareto-optimal in terms of cost and accuracy.

The Pareto-front groups the Pareto-optimal solutions meaning that a lower cost of measurements can only be obtained at the expense of lower accuracy of key variables and vice versa, higher accuracy can be obtained at the expense of a higher cost. Solution 1 was the cheapest measurement layout with 11 additional sampling points for the measurement of total sulfur concentration. Solution 7 with 17 additional measurements provided the highest accuracy and was selected as the measurement layout in this study.

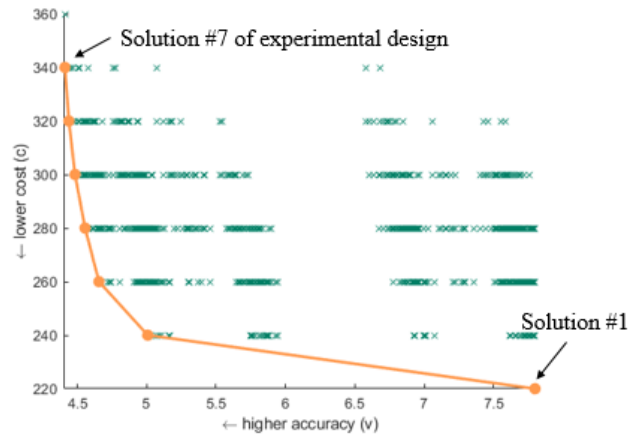


**Fig. 2:** Solutions of experimental design. Solutions are expressed in terms of cost (c) and accuracy (v). Each x represents a solution: the line filled circles represent the Pareto-front, containing all optimal solution.

Overall, the experimental design procedure proved successful in identifying Pareto-optimal measurement layouts, balancing the number of measurements and their accuracy, despite handling the given relatively complex process configuration including many possible sampling points.

### 3.2. Data Reconciliation- Quality check

A data quality check was performed for the water and, sludge streams, as well as for the gas streams. For each of them correction factor, precision improvement, gross error detection were analysed (for details of these criteria see Section 2.3.2 and section B1 in SI).

#### 3.2.1. Water and sludge streams

Data reconciliation results in reconciled (i.e. improved) values for key variables, which could be measured or unmeasured variables. The measured key variables (total sulfur mass flows) in the water and sludge streams had correction factors (Eq. 1) ranging from 1% to 15% (**Fig. 3a**). The maximum correction factors in the water line and sludge line were seen in the influent wastewater (MS3) with an 8.7% increase in the value of raw measurement and thickened primary sludge (MS62) with a 14.9% decrease in the raw measurement, respectively. This value for the feed and digested sludge of the first stage digestion (MS66 and MS68) and second stage digestion (MS75 and MS78), which have high retention time, was below 13%. Overall, the correction factors were low, reflecting that all imposed constraints (mass balances) were met by small changes in the values of raw measurements. This indicates good reliability of the raw measurements.

261 The total sulfur mass flow in the centrate of pre-dewatering (MS69) was an unmeasured key variable (i.e. both flow  
262 and total sulfur concentration were unmeasured) for which the calculated mass flow from raw data was  $15 \pm 92 \text{ kgS.d}^{-1}$ .  
263 <sup>1</sup>. Thanks to data reconciliation, the estimate of this total sulfur mass flow could be improved to  $50 \pm 40 \text{ kgS.d}^{-1}$ , which  
264 clearly implies a more precise value (data is given in section B3 in SI).

265 The precision improvement (Eq. 2) of the key variables through data reconciliation, quantifying the reduction in  
266 measurement uncertainty, is summarized in **Fig. 3b**. The average precision improvement of the key variables in the  
267 water line and the sludge line was 72%. Total sulfur mass flow in the primary sludge (MS51) had the highest precision  
268 improvement (96%). The uncertainty of the total sulfur mass flow in the primary sludge, which was defined as the  
269 ratio of the standard error to the mean, was reduced significantly: from 79% in raw measurements to 19% in reconciled  
270 value (section B3 in SI). Raw measurements from full-scale WRRFs bear uncertainties for various reasons, e.g.,  
271 influent dynamics, sampling method and measurement errors. For instance, the significant variations in the total sulfur  
272 concentrations in the primary sludge during the measurement campaign could be attributed to the different solid content  
273 of the grab samples.

274 The precision improvement of measured variables by data reconciliation is beneficial for further data handling. This  
275 improvement relies on redundancy in the measured data set that allowed variables to be estimated in several  
276 independent ways from separate sets of constraints imposed by mass balances. The improvement of the standard  
277 deviation of raw measurements by data reconciliation techniques was also reported for flow, COD and phosphorus in  
278 literature (Behnami et al., 2016; Puig et al., 2008).

279 The global test, nodal test and measurement test detected no gross errors in the total sulfur mass flows in the water line  
280 and the sludge line. It is important to note that the high uncertainty of raw measurements (average of 26%) may  
281 influence the detection of gross errors. However, in this case, there is a good agreement between measured values and  
282 reconciled values, as expressed through a low correction factor (15%). Given that the latter is lower than the 20%  
283 threshold applied by Fisher et al., (2017), it was concluded that there was a good agreement between measured and  
284 reconciled values. This constitutes an additional quality check on top of the substantial precision improvement for the  
285 water and sludge streams, and the gross error tests.

286 It can be noted that any error in mass balances could come from flow rate measurement or concentration measurement  
287 or from both. In this study, the availability of historical flow rate data over a long period permitted to perform several  
288 plant-wide flow balance reconciliations in order to check the quality of flow rate measurement prior to conducting an

intensive measurement campaign for obtaining total sulfur mass flows. These pre-evaluation steps, which are not reported in this paper, did not detect any gross error in the flow rate data. This was confirmed during data reconciliation, which allowed to reconcile both the flow rate and total sulfur concentration data. The average uncertainty of sulfur concentration measurements was higher (29%) than the one for flow rate data (9%) (Table B2, SI).

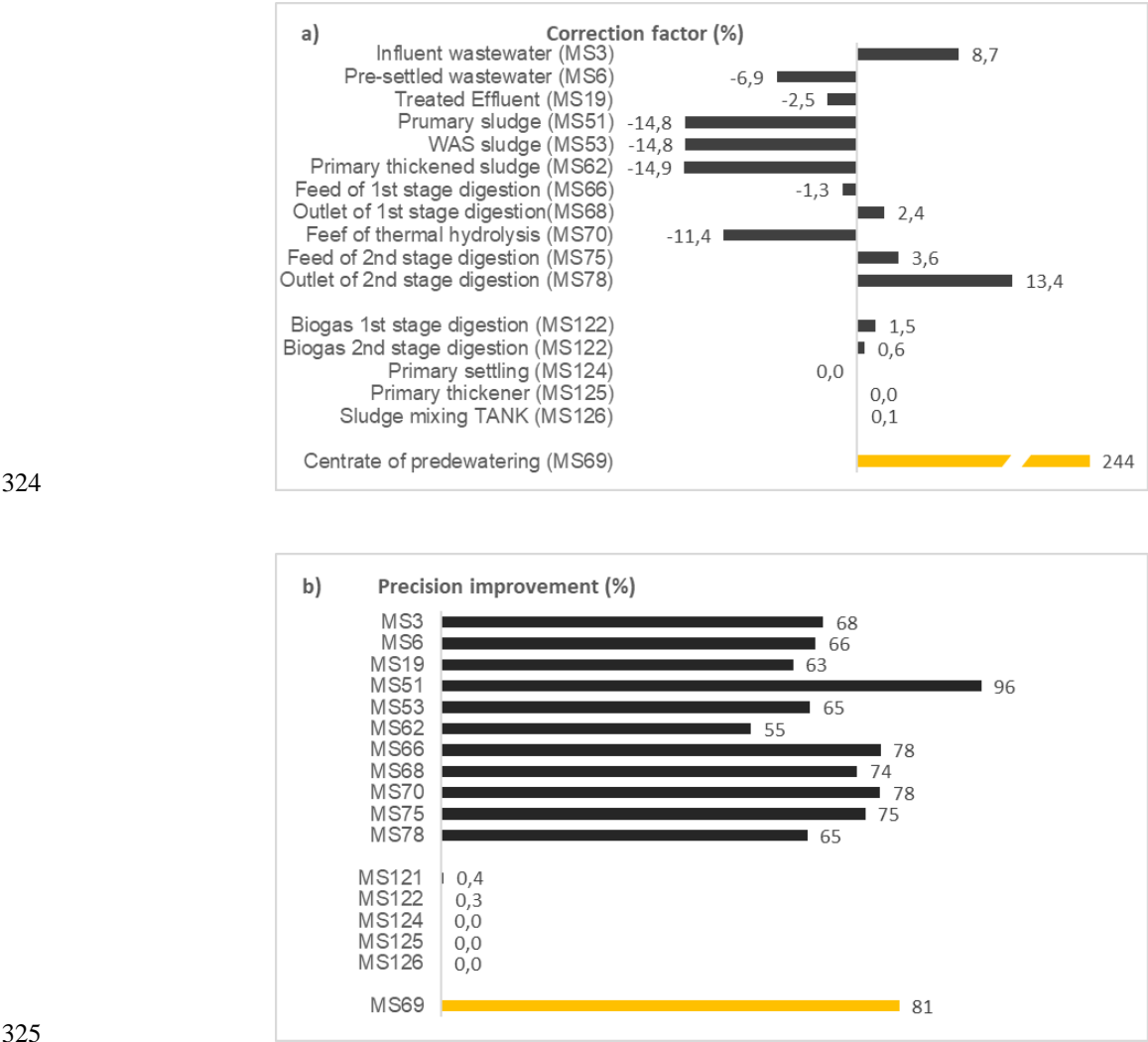
### 3.2.2. Gas streams

The values of the six measured gas streams are given in **Table B2** in SI. Five of them were key variables (MS121, MS122, MS124, MS125, MS126), which means that their value was also reconciled, i.e., calculated from other variables. However, their mean values and uncertainties hardly improved upon data reconciliation, the value of correction factor and precision improvement being less than 1% (**Fig. 3a, 3b**). The very low precision improvement indicates that data reconciliation did not really reconcile ('improve') these variables. The latter behaved as non-redundant variables in the sense that their values could not be estimated from other sets of measurements in the mass balances, even though they were indicated as redundant through the (theoretical) redundancy analysis. Such variables are referred to as "practically non-redundant" (Narasimhan and Jordache, 2000). The reason why the total sulfur mass flows in the gas streams were practically non-redundant in this study is because of their small mass flows compared to those in the water and sludge streams. In case of primary settling, for instance, the sulfur flow in the gas stream (MS124) and influent wastewater (MS3) were  $2.0 \pm 0.5 \text{ kgS.d}^{-1}$  and  $5817 \pm 947 \text{ kgS.d}^{-1}$ , respectively (for more detail see **Table B3** in SI). Indeed, the sulfur mass flows in gas streams were much smaller than the variance of the total sulfur mass flows in water and sludge streams, which for the mentioned example is 2 orders of magnitude smaller.

Because of their practical non-redundancy, gross error detection could not be applied to the measurements of total sulfur in the gas phase. Still, the measurements in these gas streams were considered to be quite reliable because of the nature of the measurement: the units were covered and the air was extracted through a ventilation pipe, in which the  $\text{H}_2\text{S}$  analyser and the flow meter were installed. The reliability of the measurement is illustrated by the relatively low uncertainty range. For instance, the measured value of the total sulfur mass flow in the biogas of second stage digestion (MS122) was  $16.9 \pm 2.5 \text{ kgS.d}^{-1}$  (**Table B3** in SI). For comparison, if this variable would not have been measured but calculated from the available measurements and prevailing mass balances, its value would have been  $58.5 \pm 50.1 \text{ kgS.d}^{-1}$ , showing 85% uncertainty. Such high uncertainties, often above 100%, were also reported by Yoshida et al. (2015) when calculating the gaseous emissions from some process units in a conventional wastewater treatment plant were calculated from other measurements using mass balances. Similar results were also reported by

317 Fisher et al. (2017) when calculating the total sulfur mass flows in the biogas of an anaerobic digester from total sulfur  
 318 measurements in the feed and outlet of the digester.

319 Despite representing smaller mass flows, gaseous sulfur streams are very important due to the problems associated  
 320 with emitted sulfur even in small quantities. They therefore need to be accurately determined by direct measurements  
 321 rather than calculated from other measurements through mass balances. Indeed, it was shown in this study that gaseous  
 322 sulfur streams cannot be accurately calculated through data reconciliation (i.e., do not qualify as key variables) because  
 323 their values are very small compared to those of sulfur loads in the liquid and sludge streams.



326 **Fig. 3:** The indicators of data reconciliation a) Correction factor b) Precision improvement for quality check of the key  
 327 variables. Measured key variables (black) and unmeasured key variables (yellow).



### 3.2.3. Effectiveness of experimental design and data reconciliation

In this work, the effectiveness of combining mass balance-based experimental design and data reconciliation procedures was demonstrated for the first time for reliable quantification of total sulfur flows and for a relatively complex WRRF. The Pareto-optimal measurement layouts put forward by the experimental design procedure showed valid for the identification of key variables. Data reconciliation and gross error detection provided better estimates for the total sulfur mass flows in the water line and the sludge line, fitting the total flow and total sulfur mass balances and characterized by a relatively high accuracy.

A balanced data set is a prerequisite for performing any type of process evaluation of full-scale WRRFs. Raw measurements are never fully accurate so the mass balances would not close perfectly without proper data reconciliation and gross error detection. For instance, model calibration and validation on erroneous data would lead to laborious and unjustified model calibrations of kinetics and stoichiometric parameters (Meijer, 2004). It is therefore, essential to reconcile the raw measurements to verify (gross) errors and improve their accuracy before being implemented.

## 3.3. Distribution of total sulfur mass flows

The plant-wide distribution of total sulfur mass flows using the reconciled data set is summarized in **Fig. 1**. In order to facilitate the comparison of streams, the total sulfur mass flows of the streams are expressed as the percentage of the total sulfur mass flows in the influent wastewater (the absolute values are given in section B3 in SI). In what follows, the total sulfur distribution in the water line, sludge line and gas streams is discussed consecutively.

### 3.3.1. Sulfur distribution in the water line

The influent wastewater (MS3, 100% total sulfur mass flow) is combined with the reject water from the sludge treatment line  $5.8 \pm 1.2\%$  and then enters the primary settling process (**Fig. 1**). Most of the total sulfur mass flow entering primary settling remained in the water line with the pre-settled wastewater (MS6) accounting for  $102 \pm 23\%$  of the total sulfur present in the influent. The high mass of sulfur in the pre-settled wastewater indicates that sulfur in the influent wastewater is mostly in soluble form. This is in agreement with the findings of Dewil et al. (2008), who reported that sulfate accounts for 99% of the sulfur in the influent wastewater.

353 After secondary treatment, comprising IFAS-based biological treatment (including anaerobic/anoxic/aerobic zones)  
354 and secondary settling, the water stream (MS19) still comprised  $96 \pm 23\%$  of the total sulfur mass flow in the incoming  
355 wastewater (MS3). This is within the range of 78-98% reported by Fisher et al. (2017), including observations from  
356 six WWTPs with different process configurations and influent wastewater flow rate. Overall, the amount of total sulfur  
357 in the water line is hardly affected by conventional (secondary) water treatment processes. Still, sulfur discharges  
358 through the dewatered sludge and gaseous emissions are critical because of their important impact on (post-treatment)  
359 process operation.

### 360 **3.3.2. Sulfur distribution in the sludge line**

361 The primary sludge (MS51) and secondary sludge (MS53) streams contained about equal amounts of total sulfur mass  
362 flows, amounting to  $3.7 \pm 0.9\%$  and  $4.5 \pm 1.1\%$  of the influent wastewater, respectively. In contrast, the distribution of  
363 sulfur during thickening was different for primary and secondary sludge, despite their similar performance in retaining  
364 total solids in the sludge line vs the filtrate - both the primary and secondary thickeners had an average thickened solid  
365 content of 60g/l. In the primary thickener, the majority of sulfur was directed to the thickened sludge (MS62,  
366  $3.1 \pm 0.8\%$ ) rather than filtrate (MS104,  $0.5 \pm 0.2\%$ ), while the secondary thickener resulted in a higher release of  
367 sulfur (57%) to the filtrate (MS55,  $2.6 \pm 0.8\%$ ) compared to thickened sludge (MS60,  $1.9 \pm 0.5\%$ ). The long HRT in  
368 the primary thickener (gravity thickening) promoted the biological formation of sulfide, which may be emitted to the  
369 hydrogen sulfide or react with present metals and form metal sulfide; hence reducing the soluble sulfur in the filtrate.  
370 As for the secondary sludge, soluble sulfur is expected to be in the form of sulfate due to the redox conditions in the  
371 aeration zone as the last step of biological treatment. Moreover, no significant microbial activity is expected in  
372 secondary thickener (rotary drums), in which physical separation between liquid and solid forms would take place. Of  
373 the total sulfur mass flow entering secondary thickening, 57% was directed to filtrate that is in agreement with the 50-  
374 68% values reported by Fisher et al. (2017). A lower value (38%) was reported in the gravity belt thickener by Dewil  
375 et al. (2008). The direction of sulfur to filtrate rather than the thickened sludge makes the dynamic thickener an  
376 important unit for reducing sulfur mass flows to the subsequent sludge treatment units (e.g., anaerobic digestion) as  
377 was also concluded by (Dewil et al., 2008). Besides thickened primary sludge and secondary sludge, the sludge buffer  
378 tank receives a fraction of thickened rain sludge (MS64,  $0.2 \pm 0.1\%$ ).

379 The contributions of different sludge sources, namely primary thickened sludge, secondary thickened sludge and  
380 thickened rain sludge in terms of total sulfur flow to sludge buffer tank were about 60%, 36% and 4%, respectively. A  
381 correlation between the primary sludge volatile solids content – as a source of organic sulfur in the form of

382 proteinaceous matter - and the hydrogen sulfide concentration in the biogas has been suggested by Erdirencelebi and  
383 Kucukhemek (2018). This study strengthens their findings through the quantification of the total sulfur flow in the  
384 primary thickened sludge, which clearly represents a considerable contribution to anaerobic digestion.

385 During the first stage digestion, the total sulfur mass flow decreased from  $5.2 \pm 1.0\%$  in the feed to  $4.8 \pm 1.0\%$  in the  
386 digested sludge, implying that sulfur mostly remained in the digested sludge. Note that the  $H_2S$  loss to biogas is reduced  
387 by microaeration, which converts  $H_2S$  to elemental sulfur. The elemental sulfur produced may partly attach to the walls  
388 and ceilings, or leave the reactor with digested sludge. Other studies have not detected significant flows of sulfur in  
389 the biogas during the studying of sulfur flows in anaerobic digestion (Dewil et al., 2008; Du and Parker, 2013; Yoshida  
390 et al., 2015). During the digestion process, the formation of metal sulfide and hydrogen sulfide are expected due to the  
391 reduction of sulfate and also degradation of organic sulfur especially from primary sludge source (Du and Parker,  
392 2013). Sulfur removed in the centrate following the pre-dewatering of the anaerobically digested sludge (MS69) was  
393  $0.9 \pm 0.7\%$  of the sulfur in the influent wastewater, showing that 18% sulfur entering pre-dewatering process being  
394 removed in the centrate. Fisher et al. (2017) reported the range of 0.5-23.1% and the range was attributed to different  
395 solid separation efficiencies of the dewatering processes. On the other hand, other studies noted minimal sulfur in the  
396 centrate of the dewatering process that was explained by the formation of insoluble metal sulfide complexes in the  
397 anaerobic digester (Dewil et al., 2008; Yoshida et al., 2015).

398 Despite a small increase in the mass of sulfur during thermal hydrolysis, which was due to the addition of reuse water  
399 containing sulfur, the total sulfur mass flow during the thermal hydrolysis remained the same with  $3.9 \pm 0.8\%$  and  
400  $4.0 \pm 0.8\%$  sulfur mass flow in the feed (MS70) and outlet (MS75) of this unit, respectively. Liu et al. (2015) studied  
401 the release of sulfur-containing odorants during the pyrolysis of sewage sludge and noted that the formation of  $H_2S$ ,  
402 the predominant odorant, at  $150^\circ C$  was insignificant. Although not yet addressed in the literature, the solubilisation of  
403 organic sulfur during thermal hydrolysis may promote the formation and emission of hydrogen sulfide to the biogas  
404 of subsequent anaerobic digestion.

405 Sulfur mass flow in the second stage of anaerobic digestion following thermal hydrolysis decreased from  $4.0 \pm 0.8\%$   
406 in the feed (MS75) to  $3.7 \pm 0.7\%$  in the digested sludge (MS78). This implies that 7% of the sulfur in the feed of  
407 second-stage digestion unit ends up in the biogas, which is considerable. The further reduction in the total sulfur flow  
408 in the sludge line through second-stage digestion is particularly interesting knowing that the degradation of sulfur  
409 species already occurred during the first-stage digestion, which indicates a possible effect of sludge thermal treatment.  
410 The hydrolysis of organic material during thermal hydrolysis especially in case of organic sulfur present in the protein

of biomass. According to Du and Parker (2013), a small fraction of protein in secondary sludge, which are likely the major contributors of organic sulfur in these streams, are not very well biodegradable in anaerobic digestion, so it could be that this source of sulfur was not degraded during the first stage digestion. While proteins are protected from the enzymatic hydrolysis during anaerobic digestion by the cell wall, thermal pre-treatment destroys the cell walls and makes the proteins accessible for biological degradation (Neyens and Baeyens, 2003). In another study, Bougrier et al. (2008) noted strong solubilisation of protein (95%) during thermal hydrolysis at 170°C and Brooks (1970) reported 40-60% solubilisation of organic material. Therefore, elimination of the rate-limiting factor in anaerobic digestion, i.e. hydrolysis, (Wilson and Novak, 2009) and the cell destruction might explain the increasing removal of sulfur in the second stage digestion.

The total sulfur mass flows removed through the centrate of post-dewatering (MS80) units was  $0.5 \pm 0.2\%$ , showing 13.6% sulfur removal through centrate of post-dewatering. This high sulfur removal was due to the solubilisation of sulfur happening during thermal hydrolysis. Overall, the total sulfur mass flow in the reject water i.e., the centrates of primary sludge and secondary sludge thickening, pre-dewatering and post-dewatering processes, accounted for  $5.8 \pm 1.2\%$  of the sulfur mass flow in incoming wastewater. The amount of total sulfur mass flow in the post-dewatered sludge (MS82) was  $3.3 \pm 0.9\%$  of the total sulfur in the influent wastewater.

The unique configuration of the two-stage anaerobic digestions with intermediate pre-dewatering, thermal hydrolysis and post-dewatering in the case study plant caused a 36% decrease in the total sulfur mass flow. Lower sulfur content in the dewatered sludge is desirable especially when the sludge is further used for co-combustion with other fuels in power stations or cement kilns, or incineration in dedicated sludge combustors because lower sulfur dioxide (SO<sub>2</sub>) is emitted with the fuel gases (Van de Velden et al., 2008; Werther and Ogada, 1999).

### 3.3.3. Gaseous sulfur streams

The amount of H<sub>2</sub>S gas streams monitored in this study accounted for  $0.7 \pm 0.1\%$  of the total sulfur mass flows in the influent wastewater (**Fig. 1**). Despite representing only small fractions of the total sulfur load, H<sub>2</sub>S emissions are critical because they cause odour nuisance, lower biogas quality and corrosion. Of the total gaseous sulfur emissions, 78% were related to the biogas of the first stage and the second stage digestion and 22% from fugitive emissions during primary settling, primary thickening, sludge buffer tank and digested sludge storage tank. Note that only the H<sub>2</sub>S emissions from these process units were measured, the H<sub>2</sub>S emission from other process units such as biological treatment was assumed negligible. No significant odour was detected in the biological treatment and clarifiers during

the measurement campaign which supports previous studies that showed the lowest emission from these units (Frechen, 2004) and justifies the decision on the 7 most important emissive units in this study. This study enabled the full quantification of gaseous sulfur emissions and their comparison.

The majority of  $\text{H}_2\text{S}$  mass flow was detected in the second stage digestion (MS122,  $0.29 \pm 0.06\%$ ) and first stage digestion (MS121,  $0.25 \pm 0.08\%$ ), which accounted for 78% of the total mass of emitted  $\text{H}_2\text{S}$ . During the measurement campaign, the range of  $\text{H}_2\text{S}$  concentration in the biogas of first stage and second stage digestion was 356-1035 ppm and 1299-1555 ppm, respectively. The high mass flow of gaseous  $\text{H}_2\text{S}$  in the second-stage digestion is in line with the above mentioned potential effect of sludge thermal treatment on  $\text{H}_2\text{S}$  formation. Two other emissive process units were primary thickener (MS125) and primary settling (MS124) with  $0.03 \pm 0.01\%$  (13-187 ppm) and  $0.09 \pm 0.03\%$  (0-22 ppm) of the total sulfur mass flows in the influent, respectively. The extent of  $\text{H}_2\text{S}$  emission from the primary settling tank depends upon both the concentration of dissolved sulfide in the incoming wastewater and the production of sulfide within the settler. Bazemo et al. (2021) estimated that majority (64%) of  $\text{H}_2\text{S}$  emission from the primary settling tank is related to dissolved sulfide formed in sewer network and present in incoming wastewater. The long HRT of the primary thickener and reductive conditions promotes the formation and subsequent emission of gaseous sulfur which was also accompanied by a drop in the ORP and pH of the samples taken from thickened sludge. The mass of emitted sulfur from sludge buffer tank (MS126) was  $0.02 \pm 0.01\%$  (60-283 ppm). It was expected to have more emission due to the presence of biomass from thickened secondary sludge that could increase the reduction of remained sulfate and organic sulfur. One explanation could be the presence of iron in the thickened rain sludge which might lead to the formation of  $\text{FeS}$  and thus less sulfur in gas streams. The lowest sulfur flow to the gas streams was detected in the digested sludge storage tank (MS127) with  $0.01\%$  (1-21 ppm).

### 3.4. Implications for research and practice

In this work, a thorough investigation of total sulfur flows was performed, identifying key sulfur flows over individual unit processes in a plant-wide context and pointing out their relative importance. The large majority of sulfur mass flow in the influent ( $96 \pm 23$ ) left the plant through the treated effluent. The sulfur in dewatered sludge accounted for  $3.3 \pm 0.9\%$ , while gaseous emissions amounted to  $0.7 \pm 0.1\%$ . Despite forming a small portion of total sulfur flow, the gaseous sulfur flows are highly undesirable and therefore require collection and treatment prior to release to the atmosphere or utilisation of biogas in co-generation.

466 The detailed quantification of gaseous streams showed that most (gaseous) H<sub>2</sub>S emissions, namely 42% of total H<sub>2</sub>S  
467 emission, were produced in the second-stage anaerobic digester, ending up in the biogas. The higher H<sub>2</sub>S emissions  
468 from the second-stage digester compared to first stage (35.7%) suggests an impact of thermal treatment on the  
469 production of H<sub>2</sub>S. Further investigation on the mechanisms and conversion of sulfur species –organic and inorganic  
470 species– are required for understanding this trend and applying control techniques as high H<sub>2</sub>S flows reduce the quality  
471 of biogas and cause corrosion problems on downstream equipment. H<sub>2</sub>S was also produced in the primary thickener  
472 (13.5%) and the primary settler (4.9%). The relatively high H<sub>2</sub>S emissions from the primary (gravity) thickener  
473 suggests the formation and emission of hydrogen sulfide during relatively long hydraulic retention time. In view of  
474 accurately modelling H<sub>2</sub>S emissions, H<sub>2</sub>S formation under anaerobic conditions thus needs to be considered to  
475 overcome the limitation of currently available H<sub>2</sub>S emission models (Santos et al., 2013).

476 When the treated sludge is used for combustion, it is beneficial to have low sulfur content in view of SO<sub>2</sub> formation  
477 upon combustion. In this regard, the secondary (drum) thickener proved effective for limiting sulfur flows towards the  
478 subsequent sludge treatment by directing majority of entering sulfur flows towards the centrate. Sludge treatment  
479 through two-stage digestion configuration with intermediate thermal hydrolysis and pre and post dewatering also  
480 considerably reduced (by 36%) the total sulfur content remained in dewatered sludge.

481 The sulfur mass flows obtained for the WRRF in this study could be used as an indication of plant-wide sulfur  
482 distribution in other WRRF facilities and configurations. Nevertheless, several specificities of WRRF in this study  
483 should be taken into account. For instance, the WRRF under study has two-stage digestion with intermediate thermal  
484 hydrolysis whereas most WRRFs have only one digester, in some cases preceded with thermal hydrolysis. As a result,  
485 the sulfur content in the final sludge stream is lower in this study.

## 486 4. Conclusions

487 Sulfur mass flows in a full-scale water resource recovery facility (WRRF) were quantified for the first time on a plant-  
488 wide level, assessing liquid, sludge and gas streams simultaneously.

- 489 - Total sulfur was demonstrated to be a conservative quantity, allowing the reliable quantification of total sulfur  
490 flows through mass balance-based experimental design and data reconciliation procedures.

- Data reconciliation and gross error detection provided better estimates for the total sulfur mass flows in the water line and the sludge line, fitting the total flow and total sulfur mass balances and characterized by a relatively high accuracy.
- The water treatment line hardly affected the incoming sulfur flows as sulfur was mostly removed through the treated effluent as sulfate. Amounting to about 8% of the sulfur in the influent wastewater, the sulfur flows in the primary and secondary sludge caused high H<sub>2</sub>S emissions in primary thickener and in both stages of anaerobic digestion. In particular, the relatively higher H<sub>2</sub>S emissions from the second-stage digester suggested an impact of the thermal treatment resulting in increased H<sub>2</sub>S production.
- Gaseous sulfur loads representing a relatively low mass are non-redundant in practice, which means that their values cannot be accurately determined from measured variables and mass balances through data reconciliation. Gaseous H<sub>2</sub>S emissions therefore need to be measured directly for obtaining reliable data.

## 5. Acknowledgements

This work was performed within the framework of the EUR H2O'Lyon (ANR-17-EURE-0018) of Université de Lyon (UdL), within the program "Investissements d'Avenir" operated by the French National Research Agency (ANR). The work of Kimberly Solon was supported by the Research Foundation Flanders (FWO) through an ERC runner-up project for Eveline Volcke and by European Union's Horizon 2020 research and innovation programme under the Marie Skłodowska-Curie Grant Agreement No. 846316 (WISEFLOW). The authors thank Sylvain Chastresse, Christophe Renner, Jonathan Coulmin, Vanessa Gromand, Ian Garcia-Fernandez from Veolia for facilitating and carrying out the measurement campaign.

## 6. References

- Appels, L., Baeyens, J., Degreè, J., Dewil, R., 2008. Principles and potential of the anaerobic digestion of waste-activated sludge. *Prog. energy Combust. Sci.* 34, 755–781.
- Baetens, D., Weemaes, M., Hosten, L., De Vos, P., Vanrolleghem, P.A., 2001. Enhanced Biological Phosphorus Removal Competition and symbiosis between SRBs and PAOs on lactate/acetate feed. *J. Exp. Bot.* 57, 3813–3824.
- Bazemo, U., Gardner, E., Romero, A., Hauduc, H., Al-Omari, A., Takacs, I., Murthy, S., Torrents, A., De Clippeleir, H., 2021. Investigating the dynamics of volatile sulfur compound emission from primary systems at a water resource recovery facility. *Water Environ. Res.* 93, 316–327.
- Behnami, A., Shakerkhatibi, M., Dehghanzadeh, R., Benis, K.Z., Derafshi, S., Fatehifar, E., 2016. The implementation of data reconciliation for evaluating a full-scale petrochemical wastewater treatment plant. *Environ. Sci. Pollut. Res.* 23, 22586–22595.

522 Bougrier, C., Delgenès, J.P., Carrère, H., 2008. Effects of thermal treatments on five different waste activated sludge  
523 samples solubilisation, physical properties and anaerobic digestion. *Chem. Eng. J.* 139, 236–244.  
524 <https://doi.org/10.1016/j.cej.2007.07.099>

525 Brooks, R., 1970. Heat treatment of sewage sludge. *Water Pollut Contr (London)* 69, 92–99.

526 Chen, Y., Cheng, J.J., Creamer, K.S., 2008. Inhibition of anaerobic digestion process: a review. *Bioresour. Technol.*  
527 99, 4044–4064.

528 Dewil, R., Baeyens, J., Roels, J., Steene, B. Van De, 2009. Evolution of total sulphur content in full scale wastewater  
529 sludge treatment. *Environ. Eng. Sci.* 26, 292–300.

530 Dewil, R., Baeyens, J., Roels, J., Steene, B. Van De, 2008. Distribution of sulphur compounds in sewage sludge  
531 treatment. *Environ. Eng. Sci.* 25, 879–886.

532 Dincer, F., Muezzinoglu, A., 2008. Odor-causing volatile organic compounds in wastewater treatment plant units and  
533 sludge management areas, in: *Journal of Environmental Science and Health - Part A Toxic/Hazardous*  
534 *Substances and Environmental Engineering*. Taylor & Francis, pp. 1569–1574.

535 Du, W., Parker, W., 2013. Characterization of sulfur in raw and anaerobically digested municipal wastewater treatment  
536 sludges. *Water Environ. Res.* 85, 124–132.

537 Erdirencelebi, D., Kucukhemek, M., 2018. Control of hydrogen sulphide in full-scale anaerobic digesters using iron  
538 (III) chloride: Performance, origin and effects. *Water SA* 44, 176–183.

539 Fisher, R.M., Alvarez-Gaitan, J.P., Stuetz, R.M., Moore, S.J., 2017. Sulfur flows and biosolids processing: using  
540 Material Flux Analysis (MFA) principles at wastewater treatment plants. *J. Environ. Manage.* 198, 153–162.

541 Fisher, R.M., Le-Minh, N., Alvarez-Gaitan, J.P., Moore, S.J., Stuetz, R.M., 2018. Emissions of volatile sulfur  
542 compounds (VSCs) throughout wastewater biosolids processing. *Sci. Total Environ.* 616–617, 622–631.

543 Frechen, F.-B., 2004. Odour emission inventory of German wastewater treatment plants-odour flow rates and odour  
544 emission capacity. *Water Sci. Technol.* 50, 139–146.

545 Frechen, F.B., 1988. Odour emissions and odour control at wastewater treatment plants in West Germany. *Water Sci.*  
546 *Technol.* 20, 261–266.

547 Galloway, J.N., Cowling, E.B., 2002. Reactive nitrogen and the world: 200 years of change. *AMBIO A J. Hum.*  
548 *Environ.* 31, 64–71.

549 Ge, H., Zhang, L., Batstone, D.J., Keller, J., Yuan, Z., 2013. Impact of iron salt dosage to sewers on downstream  
550 anaerobic sludge digesters: sulfide control and methane production. *J. Environ. Eng.* 139, 594–601.

551 Gostelow, P., Parsons, S.A., Stuetz, R.M., 2001. Odour measurements for sewage treatment works. *Water Res.* 35,  
552 579–597.

553 Guerrero, L., Montalvo, S., Huiliñir, C., Campos, J.L., Barahona, A., Borja, R., 2016. Advances in the biological  
554 removal of sulphides from aqueous phase in anaerobic processes: A review. *Environ. Rev.* 24, 84–100.

555 Guest, J.S., Skerlos, S.J., Barnard, J.L., Beck, M.B., Daigger, G.T., Hilger, H., Jackson, S.J., Karvazy, K., Kelly, L.,  
556 Macpherson, L., 2009. A new planning and design paradigm to achieve sustainable resource recovery from  
557 wastewater. *Environ. Sci. Technol.* 43, 6126–6130.

558 Gutierrez, O., Park, D., Sharma, K.R., Yuan, Z., 2010. Iron salts dosage for sulfide control in sewers induces chemical  
559 phosphorus removal during wastewater treatment. *Water Res.* 44, 3467–3475.

560 Hao, X., Wang, X., Liu, R., Li, S., van Loosdrecht, M.C.M., Jiang, H., 2019. Environmental impacts of resource  
561 recovery from wastewater treatment plants. *Water Res.* 160, 268–277.

562 Harada, H., Uemura, S., Momonoi, K., 1994. Interaction between sulfate-reducing bacteria and methane-producing



563 bacteria in UASB reactors fed with low strength wastes containing different levels of sulfate. *Water Res.* 28,  
564 355–367.

565 Jiang, G., Melder, D., Keller, J., Yuan, Z., 2017. Odor emissions from domestic wastewater: a review. *Crit. Rev.*  
566 *Environ. Sci. Technol.* 47, 1581–1611.

567 Lau, G.N., Sharma, K.R., Chen, G.H., Van Loosdrecht, M.C.M., 2006. Integration of sulphate reduction, autotrophic  
568 denitrification and nitrification to achieve low-cost excess sludge minimisation for Hong Kong sewage. *Water*  
569 *Sci. Technol.* 53, 227–235.

570 Le, H.Q., 2019. Mass-Balance-based Experimental Design and Data Reconciliation for Wastewater Treatment  
571 Processes. PhD Thesis. Ghent University.

572 Le, Q.H., Verheijen, P.J.T., van Loosdrecht, M.C.M., Volcke, E.I.P., 2018. Experimental design for evaluating WWTP  
573 data by linear mass balances. *Water Res.* 142, 415–425.

574 Lebrero, R., Bouchy, L., Stuetz, R., Muñoz, R., 2011. Odor assessment and management in wastewater treatment  
575 plants: a review. *Crit. Rev. Environ. Sci. Technol.* 41, 915–950.

576 Lebrero, R., Rangel, M.G.L., Muñoz, R., 2013. Characterization and biofiltration of a real odorous emission from  
577 wastewater treatment plant sludge. *J. Environ. Manage.* 116, 50–57.

578 Liu, S., Wei, M., Qiao, Y., Yang, Z., Gui, B., Yu, Y., Xu, M., 2015. Release of organic sulfur as sulfur-containing  
579 gases during low temperature pyrolysis of sewage sludge. *Proc. Combust. Inst.* 35, 2767–2775.

580 Lomans, B.P., Drift, C. Van Der, Pol, A., Camp, H.J.M.O. Den, van der Drift, C., Pol, A., Op den Camp, H.J.M., 2002.  
581 Cellular and molecular life sciences microbial cycling of volatile organic sulfur compounds. *Cell. Mol. Life Sci.*  
582 59, 575–588.

583 Marti, N., Ferrer, J., Seco, A., Bouzas, A., 2008. Optimisation of sludge line management to enhance phosphorus  
584 recovery in WWTP. *Water Res.* 42, 4609–4618.

585 Meijer, S.C.F., Van Der Spoel, H., Susanti, S., Heijnen, J.J., Van Loosdrecht, M.C.M., 2002. Error diagnostics and  
586 data reconciliation for activated sludge modelling using mass balances, in: *Water Science and Technology*. pp.  
587 145–156.

588 Meijer, S.C.F., 2004. Theoretical and practical aspects of modelling activated sludge processes. PhD Thesis. Delft  
589 University of Technology, The Netherlands.

590 Meijer, S.C.F., van Kempen, R.N.A., Appeldoorn, K.J., 2015. Plant upgrade using big-data and reconciliation  
591 techniques, in: *Applications of Activated Sludge Models*. IWA publishing, pp. 357–410.

592 Mihelcic, J.R., Fry, L.M., Shaw, R., 2011. Global potential of phosphorus recovery from human urine and feces.  
593 *Chemosphere* 84, 832–839.

594 Muyzer, G., Stams, A.J.M., 2008. The ecology and biotechnology of sulphate-reducing bacteria. *Nat. Rev. Microbiol.*  
595 6, 441–454.

596 Narasimhan, S., Jordache, C., 2000. Data reconciliation and gross error detection : an intelligent use of process data,  
597 *Annals of the New York Academy of Sciences*. Gulf Publishing Company, Houston, Texas, US.

598 Neyens, E., Baeyens, J., 2003. A review of thermal sludge pre-treatment processes to improve dewaterability. *J.*  
599 *Hazard. Mater.* 98, 51–67.

600 Puchongkawarin, C., Gomez-Mont, C., Stuckey, D.C., Chachuat, B., 2015. Optimization-based methodology for the  
601 development of wastewater facilities for energy and nutrient recovery. *Chemosphere* 140, 150–158.

602 Puig, S., van Loosdrecht, M.C.M., Colprim, J., Meijer, S.C.F., 2008. Data evaluation of full-scale wastewater treatment  
603 plants by mass balance. *Water Res.* 42, 4645–4655.

604 Puyol, D., Batstone, D.J., Hülsen, T., Astals, S., Peces, M., Krömer, J.O., 2017. Resource recovery from wastewater  
605 by biological technologies: Opportunities, challenges, and prospects. *Front. Microbiol.* 7, 1–23.

606 Ras, M.R., Borrell, F., Marcé, R.M., 2008. Determination of volatile organic sulfur compounds in the air at sewage  
607 management areas by thermal desorption and gas chromatography–mass spectrometry. *Talanta* 74, 562–569.

608 Roussel, J., Carliell-Marquet, C., 2016. Significance of vivianite precipitation on the mobility of iron in anaerobically  
609 digested sludge. *Front. Environ. Sci.* 4, 60.

610 Rubio-Rincón, F.J., Lopez-Vazquez, C.M., Welles, L., Van Loosdrecht, M.C.M., Brdjanovic, D., 2017a. Sulphide  
611 effects on the physiology of *Candidatus Accumulibacter phosphatis* type I. *Appl. Microbiol. Biotechnol.* 101,  
612 1661–1672.

613 Rubio-Rincón, F.J., Welles, L., Lopez-Vazquez, C.M., Nierychlo, M., Abbas, B., Geleijnse, M., Nielsen, P.H., Van  
614 Loosdrecht, M.C.M., Brdjanovic, D., 2017b. Long-term effects of sulphide on the enhanced biological removal  
615 of phosphorus: the symbiotic role of *Thiothrix caldifontis*. *Water Res.* 116, 53–64.

616 Saad, S.A., Welles, L., Lopez-Vazquez, C.M., van Loosdrecht, M.C.M., Brdjanovic, D., 2017. Sulfide effects on the  
617 anaerobic metabolism of polyphosphate-accumulating organisms. *Chem. Eng. J.* 326, 68–77.

618 Santos, J.M., Sa, L.M. de, Reis Junior, N.C., Horan, N.J., 2013. Kinetic models of hydrogen sulphide formation in  
619 anaerobic bioreactors. *Environ. Technol. Rev.* 2, 45–54.

620 Schippers, A., Jørgensen, B.B., 2002. Biogeochemistry of pyrite and iron sulfide oxidation in marine sediments.  
621 *Geochim. Cosmochim. Acta* 66, 85–92.

622 Solon, K., Jia, M., Volcke, E.I.P., 2019a. Process schemes for future energy-positive water resource recovery facilities.  
623 *Water Sci. Technol.* 79, 1808–1820.

624 Solon, K., Volcke, E.I.P., Spérandio, M., van Loosdrecht, M.C.M., 2019b. Resource recovery and wastewater  
625 treatment modelling. *Environ. Sci. Water Res. Technol.* 5, 631–642.

626 Tchobanoglous, G., Burton, F., Stensel, H.D., 2003. *Wastewater Engineering Treatment and Reuse*, fourth ed. Metcalf  
627 & Eddy, Inc, McGraw Hill, New York.

628 Van de Velden, M., Dewil, R., Baeyens, J., Josson, L., Lanssens, P., 2008. The distribution of heavy metals during  
629 fluidized bed combustion of sludge (FBSC). *J. Hazard. Mater.* 151, 96–102.

630 van der Heijden, R.T.J.M., Heijnen, J.J., Hellinga, C., Romein, B., Luyben, K.C.A.M., 1994. Linear constraint relations  
631 in biochemical reaction systems: I. Classification of the calculability and the balanceability of conversion rates.  
632 *Biotechnol. Bioeng.* 43, 3–10.

633 Visser, A., Beeksmä, I., Van der Zee, F., Stams, A.J.M., Lettinga, G., 1993. Anaerobic degradation of volatile fatty  
634 acids at different sulphate concentrations. *Appl. Microbiol. Biotechnol.* 40, 549–556.

635 Wang, J., Lu, H., Chen, G.-H., Lau, G.N., Tsang, W.L., van Loosdrecht, M.C.M., 2009. A novel sulfate reduction,  
636 autotrophic denitrification, nitrification integrated (SANI) process for saline wastewater treatment. *Water Res.*  
637 43, 2363–2372.

638 Wanner, J., Kucman, K., Ottova, V., Grau, P., 1987. Effect of anaerobic conditions on activated sludge filamentous  
639 bulking in laboratory systems. *Water Res.* 21, 1541–1546.

640 Werther, J., Ogada, T., 1999. Sewage sludge combustion. *Prog. energy Combust. Sci.* 25, 55–116.

641 Wilson, C.A., Novak, J.T., 2009. Hydrolysis of macromolecular components of primary and secondary wastewater  
642 sludge by thermal hydrolytic pretreatment. *Water Res.* 43, 4489–4498.

643 Yamamoto-Ikemoto, R., Matsui, S., Komori, T., 1994. Ecological interactions among denitrification, poly-P  
644 accumulation, sulfate reduction, and filamentous sulfur bacteria in activated sludge. *Water Sci. Technol.* 30 (11),  
645 201–210.

- 646 Yang, G., Zhang, G., Zhuan, R., Yang, A., Wang, Y., 2016. Transformations, inhibition and inhibition control methods  
647 of sulfur in sludge anaerobic digestion: a review. *Curr. Org. Chem.* 20, 2780–2789.
- 648 Yoshida, H., Christensen, T.H., Guildal, T., Scheutz, C., 2015. A comprehensive substance flow analysis of a  
649 municipal wastewater and sludge treatment plant. *Chemosphere* 138, 874–882.